INTERNATIONAL CENTER FOR NUMERICAL METHODS IN ENGINEERING

A Cooling System for a Hybrid PV/Thermal Linear Concentrator

D. Chemisana
J. Cipriano
M. Ibáñez
B. Abbdel Mesih
A. Mellor

Publication CIMNE Nº-325, October 2008

A Cooling System for a Hybrid PV/Thermal Linear Concentrator

D. Chemisana
J. Cipriano
M. Ibáñez
B. Abbdel Mesih
A. Mellor

Publication CIMNE Nº-325, October 2008

International Center for Numerical Methods in Engineering
Gran Capitán s/n, 08034 Barcelona, Spain

EUROSUN 2008
1st International Congress on Heating, Cooling, and Buildings
7th to 10th October, Lisbon - Portugal

174 - A COOLING SYSTEM FOR A HYBRID PV/THERMAL LINEAR CONCENTRATOR

D. Chemisana[1*], J. Cipriano, M. Ibáñez, B. Abbdel Mesih , A. Mellor

[1] University of Lleida, 25001 Lleida, Spain.

[*] Daniel Chemisana, daniel.chemisana@macs.udl.cat

Abstract

This paper presents the thermal evaluation of an evacuated PVT collector designed to operate under concentrated radiation (15 suns). Finite volume 3D numerical computations have been carried out in order to study the thermal characteristics of different rectangular cross section aluminium pipes and to test the performance of the PVT collector with several laminar flow rates. Experiments with the same laminar flows show the same behavior than in the numerical results.

Keywords: linear concentration, active cooling, PVT.

1. Introduction

Within the field of solar collectors, there is a group of hybrid photovoltaic/thermal (PVT) generators, which simultaneously convert sunlight into electrical and thermal energy. Electrical energy is produced by photovoltaic cells. Thermal energy is produced by means of a circulation of fluid around the hottest parts of the system (namely the photovoltaic cells). Due the difference in temperatures, heat is transferred to the fluid providing an energy source whilst cooling the cells.
PVT systems can operate under concentrated or un-concentrated light. The system analysed in this research, will operate under linear concentrated radiation.
These PV/T systems have an inherent contradiction: from the point of view of the electricity generation, the temperature of the PV cells must be kept as low as possible, which leads to low outlet temperatures of the thermal fluid, by contrast, from the thermal energy point of view high outlet temperatures are needed. Hence, a balance between PV efficiency and thermal energy production must be chosen.

1.1. Linear concentrators with active dissipation systems which generate thermal energy

In 1981 Florschuetz [4] remarked that the use of air as an active refrigeration system is not a viable alternative because of its low thermal capacity and diffusivity. He found that water is a fluid whose properties allow for a better thermal interchange and consequentially the achievement of higher concentrations without the negative effects of the temperature over the PV cell efficiency.
After this study, a group of authors developed a series of active cooling systems using water (Edenburn, O'Leary and Clements, Chenlo and Cid, Russell). Although each system used the water cooling device to optimise conditions for electricity production, none of them analyse the possibility of taking advantage of the thermal energy produced by the warming up the water.

At present, there are two principal systems which optimise both the electricity production and the thermal energy production:

- CHAPS (Combined Heat And Power Solar), developed at the Australian National University. It consists of a parabolic concentrator with a ratio of 37X which focuses radiation onto a PVT module. The module converts the radiation into thermal and electrical energy with efficiencies of 57% and 11% respectively. The prototype was initially designed as a photovoltaic system with active cooling, the idea later evolved to use the water to capture the thermal energy. Reference data of the thermal gain achieved by the collector is not mentioned in any of the reference publications for the system [5].
- BIFRES, developed at the University of Lleida, is a system which concentrates radiation by Fresnel reflection to a concentration factor of 22X. The hybrid module operates with a nominal thermal efficiency of 59%, permitting the c-Si photovoltaic cells to operate at an optimum efficiency of 11.9% [2].

Both systems positively satisfy the requirements of actively cooling the cells whilst acting as a thermal collector with acceptable efficiencies, above 50%. However, in both cases the PVT module design is not straightforward. Both groups have opted for a tube of circular cross-section appended to an absorber on which the photovoltaic cells are placed. The two systems have significant differences: the heat sink is made of aluminium in the CHAPS system and of copper in the BIFRES system, also the tube developed at the ANU is furrowed with the goal of improving convection into the fluid.
After analyzing these two systems, some improvements may arise: It is well known that rectangular sections have higher Nusselt numbers than circular or square sections. A section with a higher aspect ratio (α), permits a greater thermal interchange into the fluid, where (α) is defined as the quotient between the long and short side of the rectangle [6]. Besides, an attractive concept such as the architectural integration is not well solved in the majority of PVT systems. As a consequence of their dimensions, PVT systems are only suitable for installation on flat roofs.
In this research is proposed, with the same concentration ratio than in the other systems explained before, to reduce the dimensions of the concentrator and the absorber to facilitate the integration in buildings.

2. Numerical analysis

2.1. General specifications

The configuration of the PVT module consists of a row of photovoltaic cells with a rectangular surface area of 1cm x 1m, placed at the top of the aluminium heat sink. The encapsulation can be divided into various elements.
1.-In the surface at which concentrated radiation is received, an EVA film is applied to the cells, and high absorption glass with low iron content is used as an outer skin. This reduces deterioration of the cells and minimises the thermal losses through the top of the module.
2.- Between the cell and the heat sink a strip of electrical insulation is inserted using a double sided adhesion (Chomerics Thermattach T404). This method considerably-simplifies the adhesion process, as it simultaneously serves to insulate the cell and to fix it in right position.
3.-Finally, the lateral and underneath faces of the heat sink are thermally insulated-with a plate of temperature resistant polypropylene.

The figure 2 shows a scheme of the proposed cooling system. Concerning to the boundary conditions they must be fixed in the numerical study. In the outer upper face of the cooling device a, Neumann boundary condition of 1000W/ m^2 is applied. This represents the heat flow per unit surface area that the cells transmit to their back contact. The remaining lateral boundaries are considered to be adiabatic surfaces, assuming that the insulation is sufficiently wide to achieve this requirement. Finally, at the surfaces that represent the entry and exit of the fluid flow, the boundary conditions are fixed flow at the entrance and free flow at the exit.

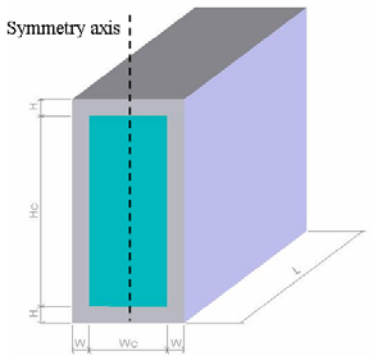

Fig.1. System scheme.

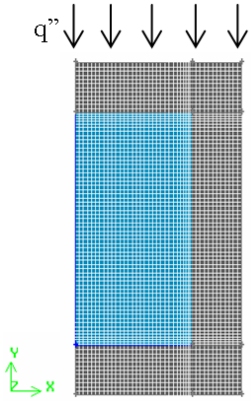

Fig.2. Simulation Scheme.

As a line of symmetry exists in the geometry (Fig.1) only half of the system will be modelled.
The tube is made of aluminium (thermal conductivity k =202W/mK). The analysed cross sections are those of the usual commercial tubes with rectangular cross section. The only requirement is a fixed section at the upper face where to accommodate the row of PV cells (1cm width). In the table 1, a summary of the analysed sections is shown. The difference among these three sections relates to the height of the section, it varies from 7 to 27 and hence the aspect ratio increases.

Table 1. Dimensions of the commercial aluminium cross sections analysed in this research

α (Hc/Wc)	H (mm)	Hc (mm)	W (mm)	Wc (mm)	L (m)
1	15	7	1.5	7	1
2.43	15	17	1.5	7	1
3.86	15	27	1.5	7	1

3. Results and discussions

3.1. Pressure losses

From an engineering point of view an important parameter is the pressure drop within the channel as this parameter determines the requirements for the pumping power. To determine the pressure drop, it is convenient to work with the friction factor of Darcy [6], defined as:

$$f \equiv \frac{-(dp/dx)D}{\rho V_m^2/2} \qquad \text{(Eq. 1)}$$

If the pressure variation is isolated from the equation 1 and integral transformation is carried, out the pressure drop is obtained as:

$$\Delta P = -\int_{p_1}^{p_2} dp = f\,\frac{\rho V_m^2}{2D}\int_{x_1}^{x_2} dx = f\,\frac{\rho V_m^2}{2D}(x_2 - x_1) \qquad \text{(Eq. 2)}$$

Where ρ is the fluid density, V_m is the mean fluid velocity, D is the hydraulic diameter and $(x_2\text{-}x_1)$ is the pipe length.
If we analyze the equation 2, it is noticed that the pressure drop is highly affected by the hydraulic diameter, which is directly linked to the shape factor (the bigger the Dh is, the smaller the AP).
Once the pressure drop is know, the pumping power can be determined as:

$$Power_{pumping} = \Delta P v_m \qquad \text{(Eq. 3)}$$

In the figure 3, a comparison the pumping power for different Reynolds numbers and the three aspect ratios previously defined is shown

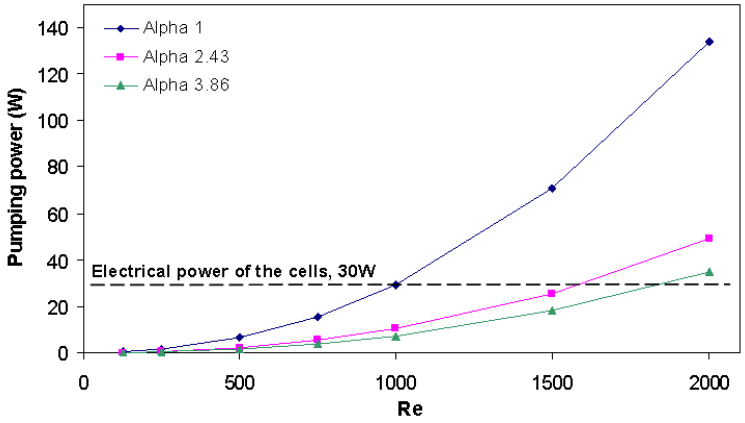

Fig.3. Pumping power.

Ignoring the effect of temperature on the cell performance, the efficiency of the electrical conversion of the cells is 20%. Therefore, for the cell surface area under investigation ($0.01 m^2$) and with an irradiation of 15000 W/m^2, the electrical power produced by the cells is predicted to be 30 W.
Taking into account the necessary pumping power and the electrical power produced by the cells, the net electrical power is defined as:

$P_{net\ electrical} = P_{elec,PV} - P_{elec,\ pumping}$ (Eq. 4)

In the figure 4, the variation of the net P with the Re and the defined aspect ratios is shown,

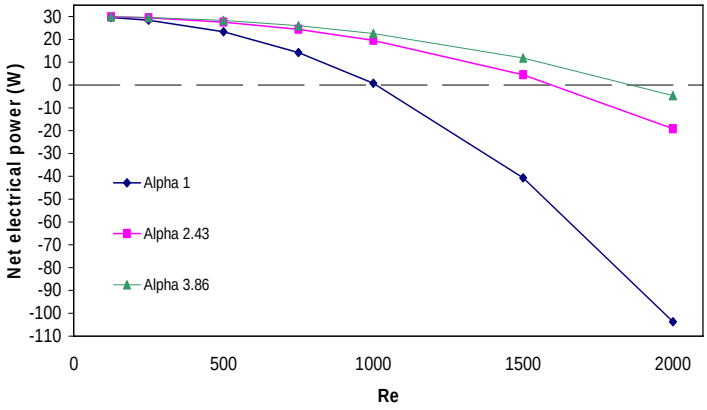

Fig.4. Net electrical power.

In the figure 4, it can be noticed that the maximum net electrical efficiency has a quadratic form, and increases with growing aspect ratio. On the other hand, the slope of the parabola in the region which describes the power in the laminar regime is much greater in tubes with smaller aspect ratio.

3.2. Distribution of temperatures

Fig. 5 shows the averaged temperatures for the channel walls and the bulk fluid:

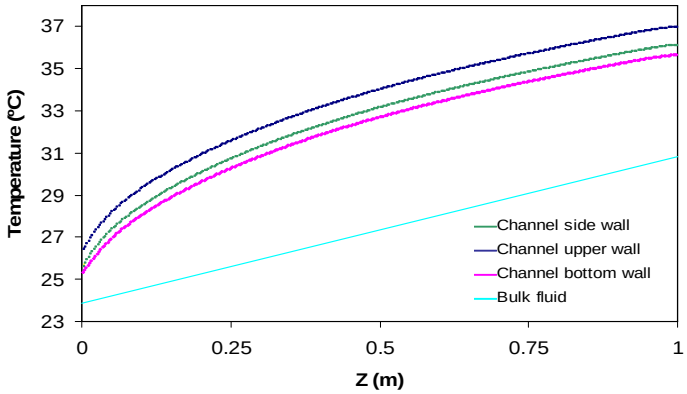

Fig. 5. Average temperature for different walls and bilk fluid, α = 2.43 and Re = 250.Example caption for figures.

A linear increase in bulk mean temperature along the tube length can be appreciated. This is a natural result of energy balance under uniform heat flux. The temperature difference between the channel walls and the fluid attains its minimum at the channel entrance region, and gradually reaches a constant value. This is in agreement with the variation of Nusselt number as will be discussed in a following section. In figure 5, the variation of the average T of each wall and the mean bulk T, obtained with the CFD simulations is shown. It can be noticed that bulk T has a linear variation and T_{walls} an exponential as it was expected.

3.3. Nusselt number

The average Nu number for each wall is obtained through the local Nu as:

$$Nu_{z,ave} = \frac{1}{L_c}\int_0^{L_c} Nu_z\, dl \qquad \text{(Eq. 5)}$$

where L_c is the width of each wall.
The overall average Nu for each aspect ratio is obtained as the proportional addition of the average Nu of each wall [1].

$$Nu_{z,perphery} = \frac{(WNu_{ave,bottom} + WNu_{ave,top} + 2HNu_{ave,side})}{2(W+H)} \quad \text{(Eq. 6)}$$

In the figure 6, the variation of the Nu with the Re, for each aspect ratio is shown

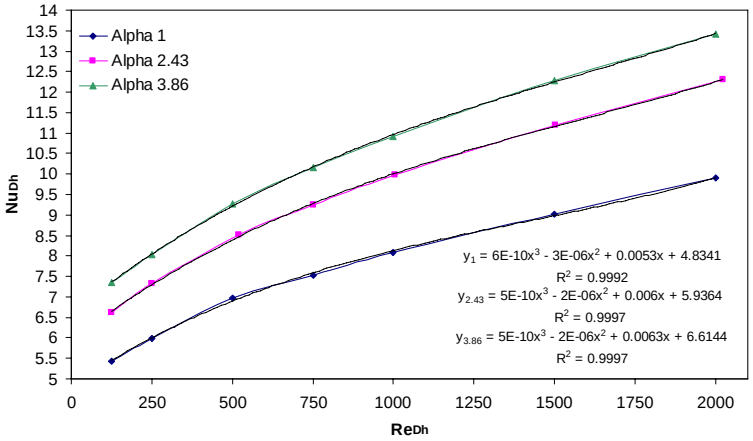

Fig.6. Average Nusselt numbers.

The thermal behaviour of the system can be understood as a function of the aspect ratio (α) and the Reynolds number. However, in order to obtain replicable results for tubes of any length, diameter, etc. A dimensionless parameter is defined as the equivalent distance of the fully developed flow from the entrance of the tube (L+, dimensionless length). This parameter has a similar definition to X+ [6], but is dependent of the total length of the tube. This parameter is known as the Graetz variable, and is defined as:

$$L+ = \frac{L/D_h}{\mathrm{Re}} \quad \text{(Eq. 7)}$$

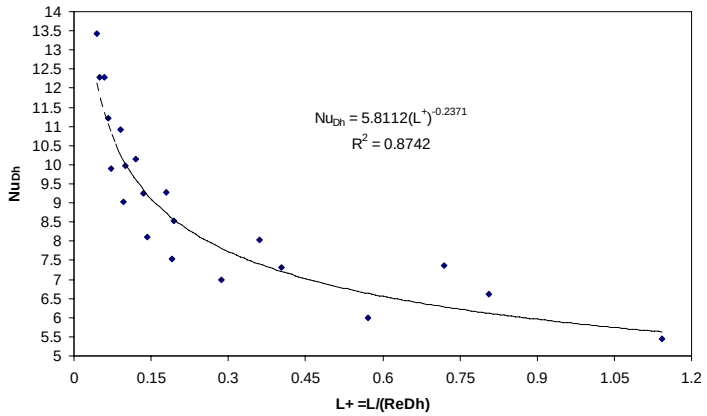

Fig. 7. Nussel general correlation.

In the figure 7 the variation of Nu with the L+ is shown. Making a minimum quadratic residual analysis a correlation can be obtained. Its mathematical expression is:

$$Nu_{Dh} = 5.811(L^{+})^{-0.237} \quad \text{(Eq. 8)}$$

3.4. Thermal resistance

The operation of the heat sink is usually evaluated by the value of the thermal resistance, defined as:

$$R_{th} = \frac{T_{w,out} - T_{in}}{q''} \quad \text{(Eq. 9)}$$

Where $T_{w,out}$ is the fluid outlet temperature and T_{in} the fluid inlet temperature.

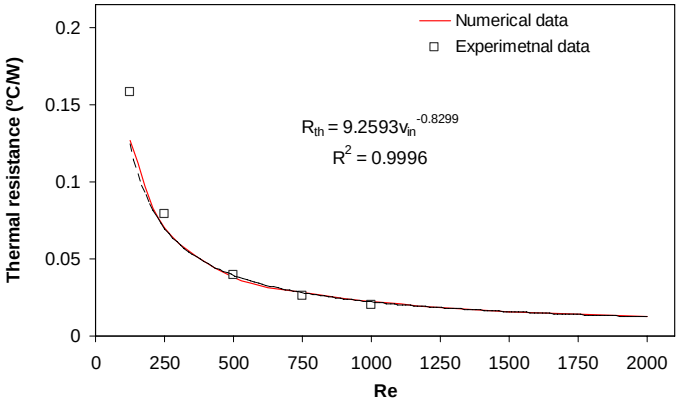

Fig. 8. Comparision of thermal resistance: numerical vs experimental (Aspect ratio = 2.43).

In literature we can find some correlations or values of the thermal resistance for linear concentrating systems:

Table 2. Thermal resistances

Authors	$1/h_c$ (m^2K/W)
Chenlo y Cid	$8.7x10^{-4}$ (Re = 5000)
Coventry.	$1.3x10^{-3}$ (Mass flow = 0.348 kg/m^2s)

Table 3. Inverse heat transfer coefficients for α=2.43.

Re	Mass flow (kg/m^2s)	$1/h_c$ (m^2K/W)
125	0.16	$1.71x10^{-3}$
250	0.31	$9.44x10^{-4}$
500	0.62	$5.14x10^{-4}$
750	0.91	$3.81x10^{-4}$
1000	1.22	$3.01x10^{-4}$
1500	1.81	$2.16x10^{-4}$
2000	2.41	$1.69x10^{-4}$

To compare with these values we should calculate the thermal resistance per unit area, obtaining the table 3.

The values of thermal resistance to the proposed sink are lower compared to those presented by Chenlo and Cid and Coventry. It should be mentioned that the values that can be compared to a greater degree [5], were acquired with the prototype working under real conditions. The values shown of the sink

design are made at the laboratory, so when comparing it is necessary to be critical quantifying differences.

5. Conclusion

The heat exchange properties of the aluminium improve increasing the aspect ratio of its cross section, in addition the pressure drop or in consequence the pumping power is higher when the hydraulic diameter (which is directly related with the cross section) is lower.
Nevertheless, a big aspect ratio implies a much more difficult mechanical procedures, suck as hydraulic connections, isolation. Moreover, is necessary to mention that the main aluminium factories don't manufacture pipes of one centimetre width with aspect ratios higher than 2.43.
Attending to this explanations, the pipe selected to be include in the PVT systems under concentration is with a cross section of $20x10cm^2$ ($\alpha = 2.43$).

Acknowledgments

This work was supported by the MCYT (Spain) (ENE2007-65410).

References

[1] P. Lee, S.V. Garimella, D. Liu. Investigation of heat transfer in rectangular microchannels. International Journal of Heat and Mass Transfer 48 (2005) 1688–1704.
[2] J.I. Rosell, X. Vallverdu, M.A. Lechon, M. Ibanez. Design and simulation of a low concentrating photovoltaic/thermal system. Energy Conversion and Management 46 (2005), 3034–3046.
[3] F. Chenlo, M. Cid, A linear concentrator photovoltaic module: analysis of non-uniform illumination and temperature effects on efficiency, Sol. Cells 20 (1987) 27–39.
[4] L.W. Florschuetz, C.R. Truman, D.E. Metzger, Streamwise flow and heat transfer distributions for jet array impingement with crossflow, J. Heat Transfer 103 (1981) 337–342.
[5] J.S. Coventry, Performance of the CHAPS collectors, Conference record, Destination Renewables– ANZSES 2003, Melbourne, Australia, 2003, pp. 144–153.
[6] F.P. Incropera, D.P. DeWitt, Fundamentals of Heat andMass Transfer, fourth ed,Wiley, New York, 1996.
[7] R.F. Russell, Uniform temperature heat pipe and method of using the same, Patent US4320246, 1982, USA.
[8] M.W. Edenburn, Active and passive cooling for concentrating photovoltaic arrays, Conference record, 14th IEEE PVSC, 1980, pp. 776–776.
[9] M.J. O'Leary, L.D. Clements, Thermal-electric performance analysis for actively cooled, concentrating photovoltaic systems, Sol. Energy 25 (1980) 401–406.